A&A 470, 1033–1041 (2007)
DOI: 10.1051/0004-6361:20066875

Astronomy & Astrophysics

The isotopic ^{6}Li/^{7}Li ratio in Centaurus X-4 and the origin of Li in X-ray binaries⋆

J. Casares[1], P. Bonifacio[2,3,4], J. I. González Hernández[1,2,3], P. Molaro[3,4], and M. Zoccali[5]

[1] Instituto de Astrofísica de Canarias, 38200 La Laguna, Tenerife, Spain
e-mail: jcv@iac.es
[2] CIFIST Marie Curie Excellence Team
[3] Observatoire de Paris, GEPI, 92195 Meudon Cedex, France
e-mail: [Piercarlo.Bonifacio;Jonay.Gonzalez-Hernandez]@obspm.fr
[4] Istituto Nazionale di Astrofisica – Osservatorio Astronomico di Trieste, via Tiepolo 11, 34143 Trieste, Italy
e-mail: molaro@ts.astro.it
[5] Pontificia Universitad Catolica de Chile, Chile
e-mail: mzoccali@puc.cl

Received 5 December 2006 / Accepted 4 May 2007

ABSTRACT

Context. Cool stars, companions to compact objects, are known to show Li abundances which are high compared to field stars of the same spectral type, which are heavily Li depleted. This may be due either to Li production or Li preservation in these systems.
Aims. Our aim is to measure the lithium isotopic ratio in the companion star of the neutron star X-ray binary Cen X-4.
Methods. We use UVES spectra obtained in years 2000 and 2004 around the orbital quadratures. The spectra are analysed with spectrum synthesis techniques and the errors estimated with Monte Carlo simulations.
Results. We measure A(Li) = 2.87 ± 0.20 and ^{6}Li/^{7}Li = $0.12^{+0.08}_{-0.05}$ at 68% confidence level. We also present updated system parameters with a refined determination of the orbital period and component masses i.e. 1.14 ± 0.45 $M_\odot$ and 0.23 ± 0.10 $M_\odot$ for the neutron star and companion, respectively.
Conclusions. In our view the low level of ^{6}Li favours Li preservation scenarios, although Li production mechanisms cannot be ruled out. In the case of preservation, no Li is freshly created in the binary, but the tidally-locked companion has preserved its original Li by some mechanism, possibly inhibited destruction due to its fast rotation.

Key words. accretion, accretion disks – stars: binaries: close – stars: individual: Cen X-4 (=V822 Cen) – X-rays: binaries

1. Introduction

Spectroscopic analysis of the companion stars to X-ray binaries provides unique information on the nature of the accreting compact objects (e.g. Casares 2001) and their formation history (Israelian et al. 1999; González Hernández et al. 2004). The subclass of Soft X-ray Transients (SXTs) provide excellent testbeds due to long periods of quiescence during which the companion star is not overwhelmed by the (otherwise) intense X-ray reprocessed disc emission (van Paradijs & McClintock 1995). The study of SXTs has led to the discovery of a large population of black holes in the Galaxy, recognized by their large mass functions (e.g. Charles & Coe 2006; Casares 2005) exceeding 3 $M_\odot$. A sizable fraction of SXTs have shown Type-I X-ray bursts and, therefore, they contain accreting neutron stars.

Cen X-4 is the nearest member of the class of neutron star SXTs with two X-ray outbursts observed in 1969 (Conner et al. 1969) and 1979 (Kaluzienski et al. 1980). V822 Cen, the optical counterpart of Cen X-4, was discovered in the course of the 1979 outburst (Canizares et al. 1980). Since 1980 it has stayed in a quiescent level at $V \simeq 18.2$ and it has been the target of intensive investigation which led to the discovery of the 15.1 h orbital period, through photometric modulations (Chevalier et al. 1989), and the determination of the companion's radial velocity curve (Cowley et al. 1988; McClintock & Remillard 1990; Torres et al. 2002). The different orbital solutions show a consistent velocity semi-amplitude (K_2 = 146–150 km s^{-1}) but a large scatter in systemic velocities which tend to converge over the years from an inital 137–234 km s^{-1} (Cowley et al. 1988; McClintock & Remillard 1990) to 184–196 km s^{-1} (Torres et al. 2002; D'Avanzo et al. 2005). The large systemic velocity and high galactic latitude (b = +24°) is consistent with Cen X-4 being a member Galaxy Halo population (Cowley et al. 1988). However, by integrating the binary motion in the Galactic gravitational potential, González Hernández et al. (2005a) propose that the binary was formed in the Galactic plane and projected into its current position by a natal kick velocity during the supernova explosion. The inclination angle has been constrained to i = 31°–54° (Shahbaz et al. 1993) and the binary mass ratio to $q = M_2/M_{\rm NS}$ = 0.17±0.06 (Torres et al. 2002) which leads to $M_{\rm NS}$ = 0.5–2.1 $M_\odot$ and M_2 = 0.04–0.58 $M_\odot$ for the masses of the neutron star and its companion.

The companion star has been classified as a K3-K7 star which must be substantially evolved in order to fill its ∼0.6 $R_\odot$ Roche lobe (see Shahbaz et al. 1993, and references therein). Detailed atmospheric parameters ($T_{\rm eff}$ = 4500 ± 100, log g = 3.9 ± 0.3) and chemical abundances of the donor star were

⋆ Based on observations collected at ESO – Paranal in programmes 065-0447 and 073-0214.

Table 1. Journal of observations.

Date	Wav. Range (Å)	Number of spectra	Exp. time (s.)	Orbital phase
25/4/2000	4780–5755	10	718	0.09–0.22
„	5837–6808	„	„	„
9/6/2000	4780–5755	10	718	0.66–0.80
„	5837–6808	„	„	„
3/4/2004	3281–4562	4	665	0.64–0.68
„	4780–5755	„	„	„
„	5837–6808	„	„	„
12/4/2004	3281–4562	4	665	0.22–0.26
„	4780–5755	„	„	„
„	5837–6808	„	„	„
16/4/2004	3281–4562	4	665	0.17–0.22
„	4780–5755	„	„	„
„	5837–6808	„	„	„
21/4/2004	3281–4562	4	665	0.19–0.23
„	4780–5755	„	„	„
„	5837–6808	„	„	„

presented in González Hernández et al. (2005b). The low gravity provides additional support for an expanded atmosphere. Furthermore, a super solar metallicity [Fe/H] = 0.23 ± 0.10 and moderately enhanced Ti and Ni is found, which supports contamination from supernova products. The companion also presents an anomalous ^{7}Li overabundance for a K type star (Martín et al. 1994; González Hernández et al. 2005b). This latter peculiarity, which is also common to the companions of several black hole binaries, has been explained by spallation reactions in the course of the X-ray outbursts (Martín et al. 1994), although other mechanisms for Li production might be possible (e.g. Yi & Narayan 1997). Alternatively, the companion could have preserved its primordial Li abundance if the binary were younger than $\simeq 10^7$ yr or depletion efficiently inhibited by the action of fast rotation (see Maccarone et al. 2005). The origin of the large ^{7}Li abundance could be addressed by measuring the isotopic ratio ^{6}Li/^{7}Li and, therefore, we have embarked in a project to obtain high resolution ($R \sim 40\,000$) spectroscopy of Cen X-4.

2. Observations and reduction

We obtained 20 spectra of Cen X-4 at the European Southern Observatory (ESO), *Observatorio Cerro Paranal*, using the 8.2 m *Very Large Telescope* (VLT), equipped with the UVES echelle spectrograph, on the nights of 25 April and 9 June 2000, covering the spectral ranges $\lambda\lambda$4780−5755 (hereafter green) and $\lambda\lambda$5837−6808 (hereafter red). A 1 arcsec slit was used resulting in a resolving power $R = 43\,000$. The exposure time was fixed to 718 s and the observations were concentrated around the quadratures to minimize the effects of orbital smearing which, for the orbital parameters of Cen X-4, is in the range 0.2−10 km s^{-1} i.e. smaller or comparable to our instrumental resolution of 7 km s^{-1}.

Sixteen more spectra of Cen X-4 were obtained on four nights in April 2004 also with UVES. The instrumental setup was identical to the 2000 observations except that the DIC1 dichroic was also employed, enabling us to obtain additional blue spectra covering $\lambda\lambda$3281−4562 (hereafter blue). Unfortunately, the count level was very low for some spectra and only 9 could be included in the analysis. The exposure time was set to 665 s which, for the phase of our observations, results in an orbital smearing ≤7 km s^{-1}. A full observing log is presented in Table 1.

We extracted the 1-dimensional spectra using optimal extraction within MIDAS ECHELLE context, and the pixel-to-wavelength calibration was obtained with the observation of a Th-Ar lamp. We compared our reduction with the ESO pipeline and found that they are comparable, except for the 2000 data where we prefer ours because it provides better statistics, in particular for the green spectra. All the spectra were flux calibrated using nightly observations of ESO flux standards. We checked the accuracy of the wavelength calibration using the λ6300.3 and λ5577.4 [OI] sky lines and found it to be precise within 0.4 km s^{-1} for the two databases.

3. Revised system parameters

Radial velocities of individual spectra were obtained through cross-correlating our red spectra ($\lambda\lambda$5837−6808) with a synthetic template computed for the stellar parameters and metallicity derived by González Hernández et al. (2005b), i.e. $T_{\rm eff}$ = 4500, $\log g$ = 3.9, [Fe/H] = 0.23, using Kurucz LTE models (Kurucz 1993). Prior to the cross-correlation, the synthetic spectrum was degraded to the resolution of our UVES data (7 km s^{-1}) and rotationally broadened by 44 km s^{-1} to match the rotational velocity of the donor star in Cen X-4 (Torres et al. 2002). A spherical rotational profile with limb-darkening $\epsilon = 0.65$ was employed (Gray 1992). The main disc emission lines (H_α, HeI λ5875 and λ6678) and interstellar/atmospheric absorptions (NaI D, λ6300) were masked from the cross-correlation. A least-squares sine wave fit to our velocity points yields the following orbital solution:

$$\gamma = 189.6 \pm 0.2 \ {\rm kms}^{-1}$$

$$P = 0.6290522 \pm 0.0000004 \ {\rm d}$$

$$T_0 = 2451660.6432 \pm 0.0005$$

$$K_2 = 144.6 \pm 0.3 \ {\rm kms}^{-1}$$

where T_0 is defined as the inferior conjunction of the optical star. The quoted uncertainties are 68 percent confidence and we have rescaled the errors so that the minimum reduced χ^2 is 1.0. Figure 1 presents our radial velocity points folded on the best fitted solution. We have also extracted velocities using our green spectra but the orbital elements obtained are identical except for a small shift of +2 km s^{-1} in the γ-velocity. Note that the velocity semiamplitude of the donor is extremely well constrained because we have concentrated our observations around the quadrature phases to minimize orbital smearing. Furthermore, the exquisite velocity accuracy of each data point (≤1 km s^{-1}) coupled with our long baseline leads to a determination of the orbital period with unprecedented accuracy.

We have also searched for evidence of period variations by comparing our T_0 with the various spectroscopic zero phases reported in literature, which we list in Table 2. Given our long baseline we were able to estimate a zero phase for years 2000 and 2004 independently. Figure 2 shows the (O−C) diagram for T_0 = 2 449 163.934 (Torres et al. 2002) and assuming a constant period at $P = 0.6290522$ d. A quadratic fit provides a significantly better description of the (O−C) diagram than a linear fit (reduced χ^2 of 4.9 vs. 9.7) and suggests that the orbital period of Cen X-4 decreases in a timescale of $P_0/\dot{P} = (1.22\pm0.31)\times10^6$ yr. Note, however, that this claim relies on the very first epoch determination, obtained by Chevalier et al. (1989) through photometric lightcurves. If this is masked out a linear fit is marginally better and hence the evidence for a period variation vanishes.

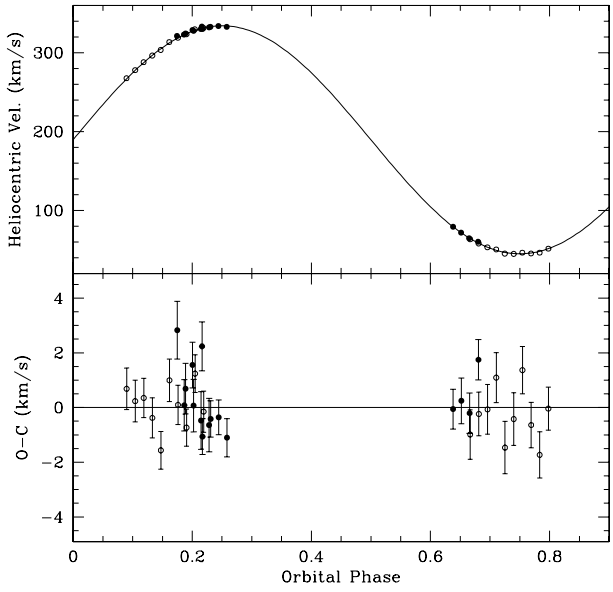

Fig. 1. Radial velocities of Cen X-4 folded on the orbital solution of Table 1 with best fitting sinusoid. Individual velocity errors are always smaller than 1 km s^{-1} and are shown in the bottom panel. Open circles represent the 2000 data and solid circles the 2004 data.

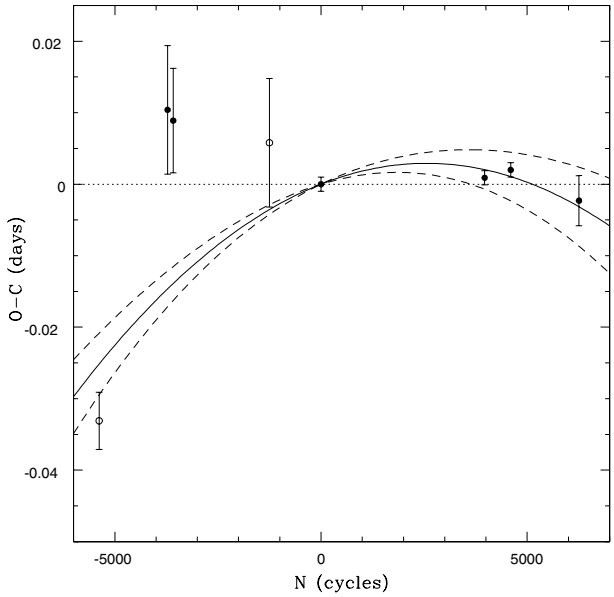

Fig. 2. The (O−C) with respect to the linear ephemeris with P = 0.6290522 d and T_0 = 2 449 163.934. Open circles mark zero phases obtained photometrically and solid circles spectroscopically. The best quadratic fit is displayed, with the 1σ uncertainty level marked in dashed lines.

Table 2. Observed zero phases.

Observed T_0 (HJD-2440000)	N (cycles)	O−C (0.001d)	Reference
5778.3420(40)	–5382	–33.1	Chevalier et al. (1989)
6822.6121(90)	–3722	10.4	Cowley et al. (1988)
6909.4198(73)	–3584	8.9	McClintock & Remillard (1990)
8376.3664(90)	–1252	5.8	Shahbaz et al. (1993)
9163.9340(10)	0	0	Torres et al. (2002)
11660.6431(10)	3969	0.9	VLT 2000
12057.5761(10)	4600	2.0	D'Avanzo et al. (2005)
13099.9113(35)	6257	–2.3	VLT 2004

Therefore, this result must be treated with caution and further observations are needed to confirm or otherwise a possible period variation in Cen X-4. Furthermore, a period decrease would be unexpected from evolutionary grounds: conservation of angular momentum leads to an increase in binary separation and mass transfer is expected to be sustained by nuclear evolution of the companion (King et al. 1996).

We subsequently produced spectral averages in the rest frame of the companion star for the 2000 and 2004 databases, using our best ephemeris. Following Marsh et al. (1994) we first computed the optimal $V_{\rm rot} \sin i$ by subtracting broadened versions of our synthetic template (in steps of 1 km s^{-1}) and minimizing the residual. We used a spherical rotational profile with linearized limb-darkening ϵ = 0.65 and obtain $V_{\rm rot} \sin i$ = 46−47 km s^{-1} for both databases, slightly higher but consistent within 1σ with Torres et al. (2002). The error is likely to be dominated by the uncertainty in ϵ which is not known for the absorption lines (Collins & Truax 1995; Shahbaz 2003). In an attempt to derive a more realistic error, we also computed the rotational broadening for the extreme cases where ϵ = 0−1 and find $V_{\rm rot} \sin i$ = 44−50 km s^{-1} or 47 ± 3 km s^{-1}. At this point we note that $V_{\rm rot} \sin i$ is known to be modulated with orbital phase because of tidal distortion of the donor star (e.g. see Casares et al. 1996). It shows a double-humped oscillation with peak-to-peak amplitude of ≃10% and maxima at the quadratures, exactly when our data were taken. Therefore, our determination is likely to be overestimated by ≃5% and hence we adopt $V_{\rm rot} \sin i$ = 44 ± 3 km s^{-1} for the sake of the system parameters determination. This value of the rotational broadening, combined with our refined K_2, implies a binary mass ratio q = 0.20 ± 0.03 (Wade & Horne 1988). We can now take our q value into the ellipsoidal solutions of Shahbaz et al. (1993) and get a much better constraint on the inclination angle of i = 33−45° (see their Fig. 3). This leads to a significant improvement in the binary masses, i.e. $M_{\rm NS}$ = 1.14 ± 0.45 $M_\odot$ and M_2 = 0.23 ± 0.10 $M_\odot$. The error budget is clearly dominated by the still large uncertainty in the inclination which needs to be refined through new high-quality ellipsoidal fits.

4. Spectral distribution

Optimal subtraction of our broadened template from the 2000 and 2004 spectral averages yields relative contributions of the donor star to the total flux at λ6400 of 78 and 89 percent, respectively. This implies that the accretion disc is dimmer in 2004, by a factor ≃2.3, with respect to 2000. In addition, the mean EW of the H$_\alpha$ emission drops from ≃40 Å in 2000 to ≃22 Å in 2004. This in turn implies that the emission line flux also decreases by a factor ≃2.1 between the two datasets. Significant variability in the accretion disc luminosity of Cen X-4 has been reported in previous works, both at short (i.e. minutes, Zurita et al. 2003) and secular (i.e. days, Chevalier et al. 1989) timescales. Furthermore, Cen X-4 is one of the brightest SXTs in quiescence, with $L_{\rm X} \simeq 4 \times 10^{32}$ erg s^{-1} and important variability (Campana et al. 2004, and references therein). It is likely that the optical changes that we observe are triggered by reprocessing of the variable X-ray flux into the accretion disc.

Figure 3 presents the average spectra of Cen X-4 in 2004, plotted in F_λ units and dereddened by $E(B-V)$ = 0.1 (Blair et al. 1984). The three spectral ranges have been rebinned into 1000 pixels and smoothed with a Gaussian bandpass of 2 pixels. We also show our synthetic template, conveniently rescaled

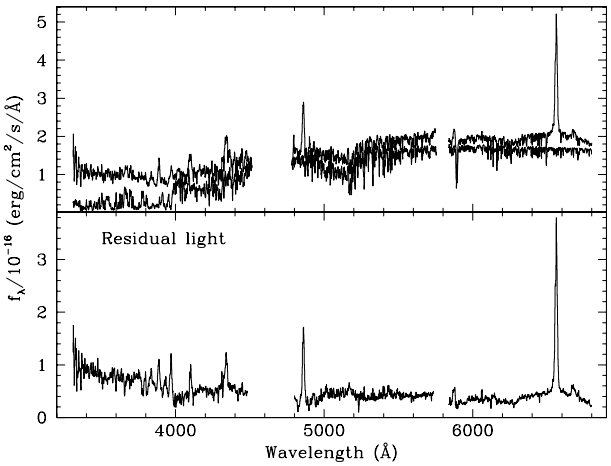

Fig. 3. *Top panel*: spectral distribution of Cen X-4, dereddened by $E_{B-V} = 0.1$, and synthetic template, scaled to 89 percent of the total flux at λ6400. *Bottom panel*: spectral distribution of the accretion disc after subtracting the synthetic template from Cen X-4.

to 89 percent of the total flux at λ6400. The bottom panel displays the residual of the subtraction which represents the spectral distribution of the accretion disc light. The continuum is well described by a standard $f_\lambda \propto \lambda^{-\alpha}$ law with $\alpha = 1.4 \pm 0.1$, in agreement with previous studies (Chevalier et al. 1988; Shahbaz et al. 1993). Furthermore, extrapolation to 2000 Å yields an excellent agreement with HST UV fluxes reported by McClintock & Remillard (2000). The spectral distribution that we find is flatter than the standard $\alpha = 2.3$ predicted for viscously heated optically thick accretion discs and suggests that irradiation of the outer disc regions may be important even in quiescence. On the other hand, the emission line fluxes yield the following Balmer decrement $H_\alpha/H_\beta/H_\gamma/H_\delta = 2.64/1/0.53/0.28$, with $F(H_\beta) = (2.14 \pm 0.06) \times 10^{-15}$ ergs cm^{-2} s^{-1} Å^{-1}. This compares very well with the standard case B recombination for $T_{\rm eff} \simeq 10^4$ K suggesting that, at the large densities typical of accretion discs ($N_{\rm e} \geq 10^{13}$ cm^{-3}), emission lines are powered by photoionization (Drake & Ulrich 1980). The same result was also obtained for the quiescent black hole SXT V404 Cyg (Casares et al. 1993). This in turn supports a scenario where the optical variability observed in both the continuum and line fluxes is triggered by reprocessing of the variable X-ray flux in the accretion disc.

5. Li abundance and ^{6}Li/^{7}Li isotopic ratio

5.1. Strategy of the analysis

The D resonance doublets of ^{6}Li and ^{7}Li are separated by about 0.16 Å (the ^{6}Li to the red), which implies that the ^{6}Li D1 line is blended with the ^{7}Li D2 line. In practice these form a unique unresolved feature even in warm slowly rotating stars, in which the feature is weak (see Smith et al. 1998 and Cayrel et al. 1999, for examples). The companion star of Cen X-4 is rotating rapidly and, to further complicate matters, the line is strongly saturated.

To analyse the Li doublet we proceed in a manner similar to that of Cayrel et al. (1999), who convincingly argued that the Li feature should be fitted with a synthetic spectrum using 5 parameters: 1) placement of the continuum, 2) and 3) abundances of the two elements 4) macroscopic broadening of the lines and 5) wavelength zero point adjustment. The stars analysed by Cayrel at al. were all slow rotators, thus the macroscopic broadening was dominated by instrumental profile and macroscopic motions in the atmosphere, in our case it is dominated by the large rotation velocity. We thus used only $V_{\rm rot} \sin i$ as fitting parameter, assuming a gaussian instrumental profile of 7 km s^{-1}, as deduced from the Th lines in the calibration arc. Thus in our case the five parameters were: 1) placement of the continuum 2) $\log(N(^6{\rm Li})/N({\rm Li_{tot}}))$ 3) $A({\rm Li})$[1] 4) $V_{\rm rot} \sin i$ 5) wavelength zero point adjustment. Of these 5 parameters 2 and 5 are correlated, quite obviously, however also 2 and 3 are strongly correlated, as we shall show below, due to the fact that the line is strongly saturated.

5.2. Model atmosphere and synthetic spectra

We used the same ATLAS LTE, plane parallel model atmosphere as in González Hernández et al. (2005b), with $T_{\rm eff} = 4500$ K, $\log g = 3.9$ and [M/H] = +0.25. The lithium doublet is heavily saturated, therefore we expect it to be seriously affected by microturbulence. The determination of the microturbulent velocity requires the measurement of both weak lines (on the linear part of the curve of growth) and strong lines (on the flat part of the curve of growth). For a rapidly rotating star, like the companion to Cen X-4, the measurement of the weak lines is impossible, therefore one has no real handle on microturbulent velocity. The need for a microturbulent velocity arises from the limitations of our one-dimensional model-atmospheres and the need to take into account the velocity fields which characterize a real stellar atmosphere. If one were to use a full three dimensional model atmosphere there should be no need to introduce such a parameter. It has long be recognized that microturbulence is not a really independent parameter, but can be calibrated as a function of effective temperature and surface gravity. One such calibration has been derived for stars in the solar neighbourhood with similar metallicity and stellar parameters (Allende Prieto et al. 2004), when applied to our adopted atmospheric parameters it provides $\xi = 0.91$ km s^{-1}. It may be questionable whether such a calibration is applicable to a star which is rapidly rotating, since it has been derived for "normal" slowly rotating dwarfs of spectral types K to F. One could however argue that meridional flows induced by rotation should be rather slow, for this rotational speed, and have a character of *macroturbulence* rather than *microturbulence*, unless the flow becomes unstable, producing small scale disturbances. Therefore we do not expect the microturbulence to be too different from $\sim$1 km s^{-1}. Our adopted value is therefore $\xi = 1$ km s^{-1}, however we shall discuss the influence of microturbulence on our results. The synthetic spectra were computed with the Linux version (Sbordone et al. 2005) of the SYNTHE suite (Kurucz 1993) We computed the emerging specific intensity for a mesh of directions, then the emerging flux was obtained by integrating the specific intensity and taking into account the stellar rotation as described e.g. in Gray (1992) and implemented by the code ROTATE of Kurucz (1993). In this way limb-darkening is automatically taken into account. We computed a small grid of synthetic spectra with 3 isotopic ratios, 3 Li abundances and 3 rotational velocities, namely $A({\rm Li}) = 2.35$, 2.55 and 3.15, $\log(N(^6{\rm Li})/N({\rm Li_{tot}})) = -4$, -1.125 and -0.301 and $V_{\rm rot} \sin i = 40$, 46 and 52 km s^{-1}. We used the same line list as in González Hernández et al. (2005b) plus the complete list of Kurucz (1993) and the TiO bands from Schwenke (1998). For Li we took into account the full HFS structure listed by Kurucz (1995) as updated by Kurucz (2006).

[1] $A({\rm Li}) = \log(N({\rm Li})/N({\rm H})) + 12$.

Table 3. Best fits for different initial parameters.

Veiling	ξ (km s^{-1})	Continuum	Shift (km s^{-1})	$V_{\rm rot} \sin i$ (km s^{-1})	A(Li)	$\log(N(^6\mathrm{Li})/N(\mathrm{Li_{tot}}))$	$N(^6\mathrm{Li})/N(^7\mathrm{Li})$
Single fits[a]							
0.22	**1**	1.07	0.36	49.6	2.97	–1.94	0.01
0.22	**1**	1.07	**0**	49.6	2.87	–1.12	0.08
0.28	**1**	1.07	**0**	49.3	3.12	–1.55	0.03
0.22	**2**	1.07	**0**	50.1	2.78	–0.97	0.12
0.22	**2**	1.07	**0**	49.3	3.05	**–4**	**10^{-4}**
Monte Carlo Simulations							
0.22	**1**	1.07 ± 0.01	**0**	49 ± 1	2.87 ± 0.20	-0.97 ± 0.19	$0.12^{+0.08}_{-0.05}$
0.22	**1**	1.06 ± 0.01	-0.42 ± 0.62	49 ± 1	2.83 ± 0.12	-1.05 ± 0.22	$0.10^{+0.07}_{-0.04}$
0.22	**2**	1.07 ± 0.01	**0**	50 ± 1	2.77 ± 0.17	-0.91 ± 0.22	$0.14^{+0.12}_{-0.06}$
0.22	**2**	1.07 ± 0.01	-0.38 ± 0.50	50 ± 1	2.73 ± 0.15	-0.88 ± 0.48	$0.15^{+0.51}_{-0.11}$
0.28	**1**	1.07 ± 0.01	**0**	49 ± 1	3.10 ± 0.22	-1.01 ± 0.16	$0.11^{+0.05}_{-0.04}$
0.28	**1**	1.07 ± 0.01	-0.77 ± 0.70	49 ± 1	3.01 ± 0.14	-1.02 ± 0.22	$0.10^{+0.08}_{-0.04}$

[a] Numbers in bold fonts correspond to parameters that have been fixed.

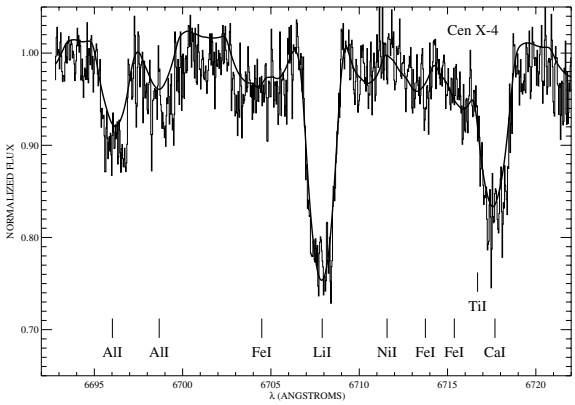

Fig. 4. Best fit to the average spectrum of year 2000, after correcting every individual spectrum from the orbital solution presented in Sect. 3. A veiling factor of 0.22 (defined as the relative contribution of the disc to the total flux) was corrected from the observed spectrum.

5.3. Line profile fitting

We used as main data set the spectra observed in year 2000, since they have higher signal-to-noise ratio with respect to those observed in year 2004 (73 vs. 34). Fits on the latter data provide, nevertheless, consistent results. We unveiled our observed spectrum by 22 percent, as derived in González Hernández et al. (2005b) for the Li region.

We wrote a χ^2 fitting code, in which the minimum is sought numerically using `MINUIT` (James 1998) and the synthetic spectra were interpolated in our grid. One useful feature of `MINUIT` is that it allows to fix any of the parameters, if required.

As a first try we fitted the whole region 6692.6−6723.5 Å where the Li line is located, and our best fit to the coadded spectrum of year 2000 is shown in Fig. 4. This fitting region is rather wide and we next attempted to fit only the region 6705.7−6709.4 Å and we find that the result does not depend on including other lines except for the Li feature. In Table 3 we show the results obtained for different values of the veiling factor, the microtrubulent velocity and leaving all 5 parameters free, or fixing at 0 km s^{-1} the velocity shift.

The main motivation for searching for solution with a fixed 0 km s^{-1} velocity shift is that our coadded spectrum has been obtained by shifting at zero velocity all the individual spectra, to better than 0.1 km s^{-1}, according to our error estimate, and hence we expect to find a zero velocity shift. To test the validity of a null velocity shift, we have performed the spectral fitting to the range $\lambda\lambda$6300−6520 Å and, indeed, obtain a zero point shift of 0 km s^{-1}. In the second place we want to test theories which predict production of ^{6}Li in low mass X-ray binaries, a positive velocity shift will tend to conceal any possible presence of ^{6}Li. Therefore a fit with a fixed 0 km s^{-1} velocity shift is useful and its result should be considered to be the "maximum" fraction of ^{6}Li compatible with the data. Finally also the results of Monte Carlo simulations (see next section) support a 0 km s^{-1} velocity shift as the most likely.

Inspection of Table 3 reveals that our derived Li abundance differs from that of González Hernández et al. (2005b). This is mainly due to the inclusion of the ^{6}Li component but also, to some extent, to the readjustment of the continuum and rotational broadening, the different adopted microturbulence and spectrum synthesis code. In fact, when one fixes the Li isotopic ratio at −4 in logarithmic scale (i.e. virtually no ^{6}Li) the A(Li) obtained is almost identical to the value reported in González Hernández et al. (2005b).

All the isotopic ratios provided in Table 3 imply very little ^{6}Li (recall that the meteoritic isotopic ratio is $\log(N(^6\mathrm{Li})/N(\mathrm{Li_{tot}})) = -1.123$). The best fit, with 1 km s^{-1} microturbulence, 0.22 veiling and fixed 0 km s^{-1} velocity shift is equivalent to ^{6}Li/^{7}Li $\simeq$ 8% and is shown in Fig. 5 as a solid line. It is remarkable that in this case the ^{6}Li content is consistent with the meteoritic abundance.

In order to get a visual impression of the change the Li isotopic ratio makes to the profiles we also show in Fig. 5 two extreme fitting profiles: one with a very low ^{6}Li content $\log(N(^6\mathrm{Li})/N(\mathrm{Li_{tot}})) = -3.5$ is shown as a dashed line, whereas another fit with very large ^{6}Li content $\log(N(^6\mathrm{Li})/N(\mathrm{Li_{tot}})) = -0.47$ is plotted as dash-dotted line. These correspond to ^{6}Li/^{7}Li = 0.03% and 50% respectively.

From Table 3 we may also deduce the impact on the derived Li abundance and isotopic ratio of the veiling factor and

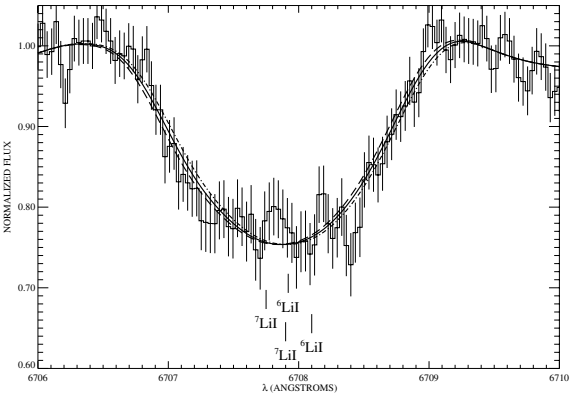

Fig. 5. Comparison of different fits to the lithium doublet, with fixed zero shift. Solid line: our best fit with all other 4 parameters free which yields $\log(N(^6\mathrm{Li})/N(\mathrm{Li_{tot}})) = -1.12$. Dashed line: fit with $\log(N(^6\mathrm{Li})/N(\mathrm{Li_{tot}})) = -3.5$ fixed. Dashed-dotted line: same with $\log(N(^6\mathrm{Li})/N(\mathrm{Li_{tot}})) = -0.47$ fixed. The spectrum of Cen X-4 was corrected from a veiling factor of 0.22.

Table 4. Impact of microturbulence and veiling factor on derived Li abundance and isotopic ratio.

Parameter	$\Delta_{A(\mathrm{Li})}$	$\Delta_{\log(N(^6\mathrm{Li})/N(\mathrm{Li_{tot}}))}$	$N(^6\mathrm{Li})/N(^7\mathrm{Li})$
Single fits			
$\Delta_\xi = +1$ km s^{-1}	-0.09	+0.15	+0.04
$\Delta_{\mathrm{veiling}} = +0.06$	+0.25	−0.43	−0.05
Monte Carlo Simulations			
$\Delta_\xi = +1$ km s^{-1}	–0.10	+0.06	+0.02
$\Delta_{\mathrm{veiling}} = +0.06$	+0.23	–0.04	–0.01

microturbulent velocity. We used the estimate of the veiling factor uncertainty by González Hernández et al. (2005b). For the reader's convenience the resulting uncertainties in A(Li), logarithmic ^{6}Li fraction and ^{6}Li/^{7}Li ratio are provided in Table 4, which has been estimated for the case where the shift is fixed at 0 km s^{-1}. Since González Hernández et al. (2005b) assumed a microturbulent velocity of 2 km s^{-1}, we have also quantified the effect of the microturbulence on the metallicity. We found that the metallicity decreases 0.1 dex for an increase of 0.25 km s^{-1}. This result is not surprising, since only strong Fe I lines could be analysed due to the large rotational velocity of the secondary star.

5.4. Confidence intervals

Although we have used χ^2 fitting, it is clear that all the theorems which allow to derive errors and confidence limits from χ^2 do not apply to the case of spectra, since adjacent pixels are always correlated, as pointed out by Cayrel et al. (1999) and Caffau et al. (2005). However, confidence limits can be reliably estimated using Monte Carlo techniques. To this end we performed Monte Carlo simulations by injecting Poisson noise, according to the standard deviations used in the fitting, into the best fitting synthetic spectrum and performing the fit with the same code used for the observed spectrum, for over 50 000 samples.

The results of four such simulations are given in the last six lines of Table 3. We would like to stress that the Monte Carlo simulations yield no significant dependence of the derived isotopic ratios on the values adopted for the microturbulent velocity

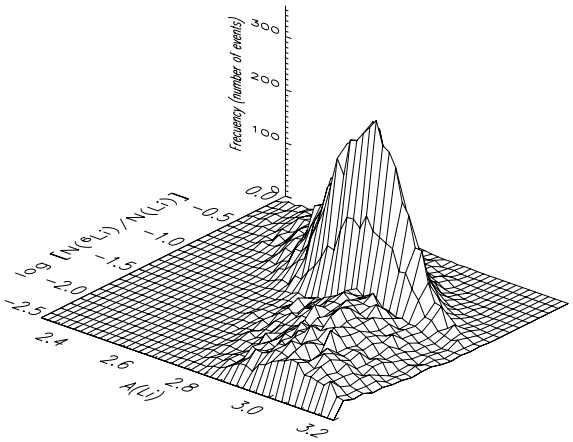

Fig. 6. 3D view of the histogram of Monte Carlo events with respect to Li isotopic ratio and total Li abundance for the model with $\xi = 1$ km s^{-1}, shift = 0 km s^{-1} (fixed) and veiling of 0.22.

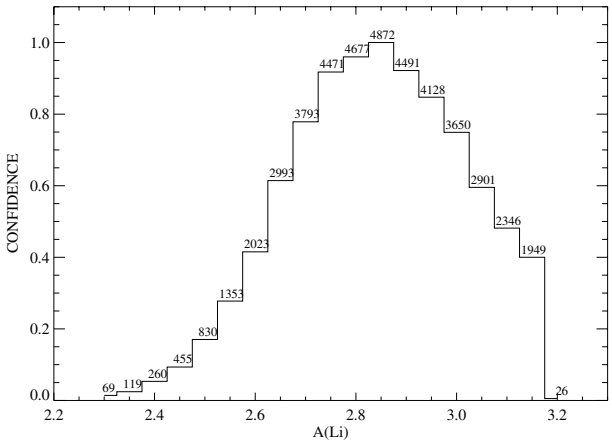

Fig. 7. Histogram of Monte Carlo events with respect to total Li abundance for the model with $\xi = 1$ km s^{-1}, shift = 0 km s^{-1} and veiling of 0.22.

and veiling factor, and are all consistent within 1-σ. The two dimensional histogram with respect to isotopic ratio and A(Li) of the simulation with $\xi = 1$ km s^{-1} and a fixed 0 km s^{-1} velocity shift, is shown in Fig. 6. The strong correlation of the two parameters is clear and results from the fact that the line is strongly saturated. The higher the ^{6}Li fraction and the more the line is desaturated, thus allowing to reach the observed equivalent width with a lower A(Li). In Fig. 8 a countour plot of the same histogram is shown. From this distribution one may estimate the area which encloses roughly 68% of the Monte Carlo samples, which may be taken as akin to 1σ for normal distributions. We find that the highest Li isotopic ratio compatible with the observations at 1σ is $\log(N(^6\mathrm{Li})/N(\mathrm{Li_{tot}})) = -0.78$ which corresponds to $N(^6\mathrm{Li})/N(^7\mathrm{Li}) = 0.20$. In fact 68% of the events are bounded by the following limits $N(^6\mathrm{Li})/N(\mathrm{Li_{tot}}) = 0.07-0.16$ and A(Li) = 2.67−3.07. Therefore, we can claim a 1σ detection of the Li isotopic ratio in Cen X-4 with $N(^6\mathrm{Li})/N(^7\mathrm{Li}) = 0.12^{+0.08}_{-0.05}$ and A(Li) = 2.87 ± 0.20. The most likely value for the Li abundance and its uncertainty was infered from the histogram extracted from the Monte Carlo simulations which is shown in Fig. 7. Note that, although the most probable value of A(Li) of the distribution coincides with the value found by the best single fit, the corresponding isotopic ratio is slightly different.

It is interesting to note that in both the Monte Carlo simulations done leaving all five parameters free, the mean value of

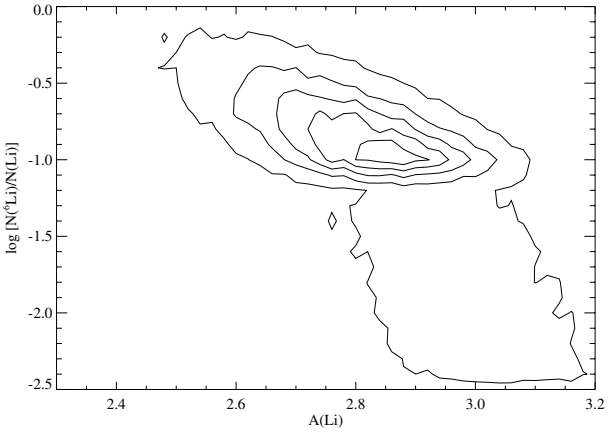

Fig. 8. Contour plot of the histogram of Monte Carlo events with respect to Li isotopic ratio and total Li abundance for the model with $\xi = 1$ km s^{-1}, shift = 0 km s^{-1} and veiling of 0.22.

the velocity shift is consisten with 0 km s^{-1}, within 1 standard deviation. In our view this strongly argues in favour of fixing at 0 km s^{-1} the velocity shift.

6. Adopted *A*(Li) and isotopic ratio

All the results of our fits and Monte Carlo simulations are listed in Table 3, whereas Table 4 summarises the impact of the veiling and microturbulent velocity.

We have already discussed the issue of veiling factor and microturbulent velocity and from our point of view the best choice is 0.22 veiling factor and 1 km s^{-1} microturbulent velocity. Concerning the velocity shift we believe that the results of the Monte Carlo simulation and the process of optimal coaddition of the spectra adopted, strongly suggest that this parameter should be fixed at 0 km s^{-1}. We are left to chose between two possible couples of values for A(Li) and $\log(N(^6\mathrm{Li})/N(\mathrm{Li_{tot}}))$: the best fit with a fixed 0 km s^{-1} velocity shift or the result of the corresponding Monte Carlo simulation. It is reassuring that the value of A(Li) is the same in both cases. The difference in isotopic ratio is small and boils down to ^{6}Li/^{7}Li = 8% for the direct fit or ^{6}Li/^{7}Li = 12% from the Monte Carlo simulation. Our discussion would not change if we adopted one or the other. However we decided to adopt the result of the Monte Carlo simulation. We believe that in a situation like this, with a minimum with a complex topology, and strongly correlated parameters, the Monte Carlo simulation does a better job in estimating the most likely parameters.

We also note that <4% of the events have $N(^6\mathrm{Li})/N(\mathrm{Li_{tot}}) > 0.4$ which defines a 3-σ upper limit to the ^{6}Li abundance of $N(^6\mathrm{Li})/N(^7\mathrm{Li}) < 0.66$.

7. Discussion

The Li abundance in the companion of Cen X-4 is known to be high (Martín et al. 1994; González Hernández et al. 2005b), and is confirmed by the present result of A(Li) = 2.87. The relevant aspect is that this value is higher of what expected for a cool K star, in which the convective zone is deep enough to destroy the surface Li. This characteristic is shared by other companions in X-ray binaries. Li detections have been reported in the companion stars to several SXTs, namely V404 Cyg (Martín et al. 1992), A0620-00 (Marsh et al. 1994), GS 2000+25 (Filippenko et al. 1995) and Nova Mus (Martín et al. 1996).

The surprising high abundance of Li observed in the cool companions of compact objects has been taken as an evidence of local Li production connected to the presence of relativistic particles around the compact objects. These are binary systems in which a compact object, a neutron star or a black hole, is accreting matter from the companion and Li production can occur either in the accretion flow or on the surface of the companion, but through processes associated with the accretion (see Guessoum & Kazanas 1999, and references therein). Proposed physical mechanisms are $\alpha - \alpha$ fusion in the accretion flow (Yi & Narayan 1997) or spallation of CNO elements by neutrons, on the star surface (Guessoum & Kazanas 1999). This leads to the prediction that other light nuclei such as ^{6}Li, Be and B must be synthesized besides ^{7}Li, the amount depends on the details of the accretion process.

However, Li in these systems is never found in excess of the presently cosmic, i.e. meteoritic value, A(Li) = 3.3 which would be an unambiguous signature of fresh Li production. Thus it has also been suggested that instead of Li production we are dealing with the supression of the destruction mechanism, which is normally very efficient for late type stars. Theoretically rotation has been shown to counteract Li depletion and some evidence of reduced Li depletion has been found in tidally locked binaries in open clusters. Martín & Claret (1996) showed that high enough rotational velocities may inhibit Li depletion in the atmospheres of such late-type stars. On the contrary, Pinsonneault et al. (1990) have found that the effects of high rotational velocities on the Li depletion processes are small and these effects are not resposible for the Li abundance dispersion in Pleiades K-dwarfs with similar effective temperatures and masses, discarding a clear correlation between non-projected rotational velocities (obtained from photometric periods) and Li abundances (King et al. 2000). More recently, Maccarone et al. (2005) have argued that inhibited Li destruction, due to tidally locked rotation of the companion stars, could explain the large abundances observed in SXTs. X-ray binaries spend several Gyr of their lifetimes as tidally locked binaries and it is only when they come into the Roche-lobe contact that some Li depletion, through mass transfer, starts. Cataclysmic variables, which are systems related to the SXT, do not show the presence of Li. This fact has been taken as evidence of Li production in the SXT (Martín et al. 1995). However, Maccarone et al pointed out that cataclysmic variables have longer lifetimes compared with the systems ending with a black hole or a neutron star and that the companions in cataclysmic variables are not tidally locked for most of their evolution prior to the Roche lobe contact phase. These differences could explain the non detection of Li in the companions of cataclysmic variables.

In Table 5 we list the *EW*s (corrected for veiling of the accretion disc) and Li abundances of several SXTs, together with the stellar rotation $V_{\rm rot}$, binary inclination (based on ellipsoidal model fits) and spectral type of their companion stars, as reported in the papers listed in Col. 8. A(Li) values are taken from the following works: Martín et al. (1996) for V404 Cyg, GU Mus and GS2000+25; González Hernández et al. (2004) for A0620-00 and González Hernández et al. (2006) for XTE J1118+480. Upper limits to A(Li) have also been computed for GRO J0422+32 and N. Oph 77 through the code MOOG (Sneden 1973) using the reported *EW*s and $T_{\rm eff}$ of companion stars. Note that Li abundances in this table do not consider ^{6}Li, except for the case of Cen X-4. $V_{\rm rot}$ is calculated from the measured rotational broadening $V_{\rm rot} \sin i$ and the inclination. Table 5 shows that there is no obvious correlation between A(Li) and $V_{\rm rot}$ but do seems to be a connection with the spectral type of the star: Li is

Table 5. Li detection in SXTs.

System	$V_{\rm rot} \sin i$ (km s^{-1})	i (deg.)	$V_{\rm rot}$ (km s^{-1})	Spectral Type	EW Li (Å)	A (Li)	Reference[a]
J1118+480	114 ± 4	68 ± 2	123 ± 5	K5-7VI	<0.16	<1.8	(1, 2)
J0422+32	90^{+22}_{-27}	45 ± 2	127 ± 36	M2-4V	<0.21	<1.62	(3, 4)
N. Oph 77	50^{+17}_{-23}	70 ± 10	53 ± 23	K5-7IV	<0.37	<2.96	(5, 6)
GS2000+25	86 ± 8	65 ± 9	95 ± 11	K3-6V	0.150 ± 0.090	2.20 ± 0.50	(7, 8)
GU Mus	106 ± 13	54 ± 2	131 ± 16	K3-K4V	0.420 ± 0.060	3.00 ± 0.50	(9, 10)
V616 Mon	93 ± 4	41 ± 3	142 ± 11	K2V	0.245 ± 0.030	2.31 ± 0.21	(11,12)
V404 Cyg	41 ± 1	55 ± 4	50 ± 3	K0IV	0.290 ± 0.030	2.70 ± 0.40	(13, 14)
Cen X-4	44 ± 3	40 ± 7	68 ± 11	K4IV	0.440 ± 0.025	2.87[b] ± 0.20	(15,16)

[a] (1) Orosz (2001); (2) Gelino et al. (2006); (3) Harlaftis et al. (1999); (4) Gelino & Harrison (2003); (5) Harlaftis et al. (1997); (6) Remillard et al. (1996); (7) Harlaftis et al. (1996); (8) Callanan et al. (1996); (9) Casares et al. (1997); (10) Gelino et al. (2001a); (11) Marsh et al. (1994); (12) Gelino et al. (2001b); (13) Casares & Charles (1994); (14) Shahbaz et al. (1994); (15) This paper. (16) Shahbaz et al. (1993). [b] Note that in this case the Li abundance has been derived taking into account the presence of ^{6}Li, at variance with what done for the other stars. A fit to the data assuming no ^{6}Li would provide an abundance higher by 0.12 dex.

only detected in companions with spectral type earlier than K5, suggesting that the depth of the convection layer seems to be an important factor. This can be taken as circumstantial support to preservation models.

A measurement to the ^{6}Li/^{7}Li ratio can, in principle, discriminate between production or preservation scenarios. This is because $\alpha + \alpha$ fusion reactions occurring in the inner region of an accretion disc containing helium would produce significant amount of ^{6}Li beside ^{7}Li and ^{7}Be which decays into ^{7}Li with a lifetime of 76 days. Unfortunately, there are no computations of $\alpha + \alpha$ reactions in accretion discs with realistic (solar) abundances. Guessoum et al. (1997) examined the nuclear reactions that occur in the inner regions of accretion discs composed of pure helium. They computed the gamma-ray lines resulting from ^{7}Li and ^{7}Be deexcitation lines which produce a feature at about 0.450 MeV and, incidentally, might have produced the 0.5 Mev emission feature observed in Nova Muscae. They conclude that the Li isotopic ratio is expected to be in the range $0.1 < N(^6\mathrm{Li})/N(^7\mathrm{Li}) < 10$ for ion temperatures of the plasma varying from $KT_i = 3$ MeV upto 50 MeV (Guessoum et al. 1997). Our analysis shows that $N(^6\mathrm{Li})/N(^7\mathrm{Li}) = 0.12^{+0.08}_{-0.05}$ and is consistent with the computations for ion temperatures ∼4.3 MeV. Therefore, our value cannot rule out Li production models, however we stress that the low level of ^{6}Li is remarkable. This, together with the possible correlation between A(Li) and spectral types and the non detection of a single X-ray binary with supermeteoritic A(Li), seems to support Li preservation scenarios. We also note that a new evolutionary picture has recently been proposed by Ivanova (2006) where LMXBs are powered by mass transfer from pre-main sequence donors. This would help to explain the roughly primordial abundance of Li in Cen X-4 through youth and, hence, our value of the isotopic ratio. Clearly, in order to confirm our result, new computations of $\alpha + \alpha$ fusion and spallation reactions in accretion discs with solar composition are required.

Acknowledgements. Use of the MOLLY and DOPPLER software developed by T. R. Marsh is gratefully acknowledged. We are grateful to H.-G. Ludwig for interesting discussions on the role of microturbulence and its possible connection to rotation. P.B. and P.M. acknowledge support from MIUR-PRIN grant 2004025729 (P.I. M. Busso). P.B. and J.I.G.H. acknowledge support from EU contract MEXT-CT-2004-014265 (CIFIST). J.C. akcnowledges support by Spanish MCYT grant AYA2002-0036.

References

Allende Prieto, C., Barklem, P. S., Lambert, D. L., & Cunha, K. 2004, A&A, 420, 183
Blair, W. P., Raymond, J. C., Dupree, A. K., et al. 1984, ApJ, 278, 270
Caffau, E., Bonifacio, P., Faraggiana, R., et al. 2005, A&A, 441, 533
Callanan, P. J., Garcia, M. R., Filippenko, A. V., McLean, I., & Teplitz, H. 1996, ApJ, 470, L57
Campana, S., Israel, G. L., Stella, L., Gastaldello, F., & Mereghetti, S. 2004, ApJ, 601, 474
Casares, J. 2001, in Binary stars: Selected Topics on Observations and Physical processes, ed. F. C. Lázaro, & M. J. Arévalo, Lect. Notes Phys., 563, 277
Casares, J. 2005, in The Many Scales of the Universe - JENAM 2004 Astrophysics Reviews, ed. J. C. del Toro Iniesta et al. (Kluwer Academic Publishers), in press [arXiv:astro-ph/0503071]
Casares, J., & Charles, P. A. 1994, MNRAS, 271, L5
Casares, J., Charles, P. A., Naylor, T., & Pavlenko, E. P. 1993, MNRAS, 265, 834
Casares, J., Mouchet, M., Martínez-Pais, I. G., & Harlaftis, E. T. 1996, MNRAS, 282, 182
Casares, J., Martín, E. L., Charles, P. A., Molaro, P., & Rebolo, R. 1997, NewA, 1, 299
Cayrel, R., Spite, M., Spite, F., et al. 1999, A&A, 343, 923
Charles, P. A., & Coe, M. J. 2006, in Compact Stellar X-ray Sources, ed. W. H. G. Lewin, & M. van der Klis, Cambridge Astrophysics Series No. 39 (CUP), 215
Chevalier, C., Ilovaisky, S. A., van Paradijs, J., Pedersen, H., & van der Klis, M. 1989, A&A, 210, 114
Collins, G. W. II, & Truax, R. J. 1995, ApJ, 439, 860
Conner, J. P., Evans, W. D., & Belian, R. D. 1969, ApJ, 157, L157
Cowley, A. P., Hutchings, J. B., Schmidtke, P. C., et al. 1988, AJ, 95, 1231
D'Avanzo, P., Campana, S., Casares, J., et al. 2005, A&A, 444, 905
Drake, S. A., & Ulrich, R. K. 1980, ApJS, 42, 351
Eggleton, P. P., Bailyn, C. D., & Tout, C. A. 1989, ApJ, 345, 489
Filippenko, A. V., Matheson, Th., & Barth, A. J. 1995, ApJ, 455, L139
Garcia, M. R., Bailyn, C. D., Grindlay, J. E., & Molnar, L. A. 1989, ApJ, 341, L75
Gelino, D. M., & Harrison, T. E. 2003, ApJ, 599, 1254
Gelino, D. M., Harrison, T. E., & McNamara, B. J. 2001a, AJ, 122, 971
Gelino, D. M., Harrison, T. E., & Orosz, J. A. 2001b, AJ, 122, 2668
Gelino, D. M., Balman, Ş., Kizloglu, Ü., et al. 2006, ApJ, 642, 438
González Hernández, J. I., Rebolo, R., Israelian, G., et al. 2004, ApJ, 609, 988
González Hernández, J. I., Rebolo, R., Peñarrubia, J., Casares, J., & Israelian, G. 2005a, A&A, 435, 1185
González Hernández, J. I., Rebolo, R., Israelian, G., Casares, J., et al. 2005b, ApJ, 630, 495
González Hernández, J. I., Rebolo, R., Israelian, G., et al. 2006, ApJ, 644, L49
Gray, D. F. 1992, The observation and Analysis of Stellar Photospheres (CUP), 20
Greenstein, J. L., & Saha, A. 1986, ApJ, 304, 721
Guessoum, N., Kazanas, D., & Kozlovsky, B. 1997, Proceedings of the 25th International Cosmic Ray Conference, Durban, South Africa, July 30−August 6, 1997, ed. M. S. Potgieter et al. (Wesprint, Potchefstroom, Space Research Unit, 1997), 145
Guessoum, N., & Kazanas, D. 1999, ApJ, 512, 332
Harlaftis, E. T., Horne, K., & Filippenko, A. V. 1996, PASP, 108, 762
Harlaftis, E. T., Steeghs, D., Horne, K., & Filippenko, A. V. 1997, AJ, 114, 1170
Harlaftis, E. T., Collier, S., Horne, K., & Filippenko, A. V. 1999, A&A, 341, 491
Israelian, G., Rebolo, R., Basri, G., Casares, J., & Martín, E. L. 1999, Nature, 401, 142

Ivanova, N. 2006, ApJ, 653, L1371
James, F. 1998, MINUIT, Reference Manual, Version 94.1, CERN, Geneva, Switzerland
Kaluzienski, L. J., Holt, S. S. & Swank, J. H. 1980, ApJ, 241, 779
King, A. R., Kolb, U., & Burderi, L. 1996, ApJ, 464, L127
King, J. R., Krishnamurthi, A., & Pinsonneault, M. H. 2000, ApJ, 119, 859
Kurucz, R. L. 1993, CDROM 13, 18
Kurucz, R. L. 1995, ApJ, 452, 102
Kurucz, R. L. 2006, http://kurucz.harvard.edu/atoms/0300
Maccarone, T. J., Jonker, P. G., & Sils, A. I. 2005, A&A, 436, 671
Marsh, T. R., Robinson, E. L., & Wood, J. H. 1994, MNRAS, 266, 137
Martín, E. L., & Claret, A. 1996, A&A, 306, 408
Martín, E. L., Rebolo, R., Casares, J., & Charles, P. A. 1992, Nature, 358, 129
Martín, E. L., Rebolo, R., Casares, J., & Charles, P. A. 1994, ApJ, 435, 791
Martín, E. L., Casares, J., Charles, P. A., & Rebolo, R. 1995, A&A, 303, 785
Martín, E. L., Casares, J., Molaro, P., Rebolo, R., & Charles, P. A. 1996, NewA, 1, 197
McClintock, J. E., & Remillard, R. A. 1990, ApJ, 350, 386
McClintock, J. E., & Remillard, R. A. 2000, ApJ, 531, 956
Orosz, J. A. 2001, Astron. Telegram, 67, 1
Pinsonneault, M. H., Kawaler, S. D., & Demarque, P. 1990, ApJS, 74, 501
Remillard, R. A., Orosz, J. A., McClintock, J. E., & Bailyn, C. D. 1996, ApJ, 459, 226
Sbordone, L., Bonifacio, P., Castelli, F., & Kurucz, R. L. 2004, MSAIS, 5, 93
Schwenke, D. M. 1998, Chemistry and Physics of Molecules and Grains in Space, Faraday Discuss. 109 (The Faraday division of the Royal Society of Chemistry, London), 321
Shahbaz, T. 2003, MNRAS, 339, 1031
Shahbaz, T., Naylor, T., & Charles, P. A. 1993, MNRAS, 265, 655
Shahbaz, T., Ringwald, F. A., Bunn, J. C., et al. 1994, MNRAS, 271, L10
Smith, V. V., Shetrone, M. D., & Keane, M. J. 1999, ApJ, 516, L73
Sneden, C. 1973, Ph.D. Thesis, Univ. Texas, Austin
Torres, M. P., Casares, J., Martínez-Pais, I. G., & Charles, P. A. 2002, MNRAS, 334, 233
van Paradijs, J., & McClintock, J. E. 1995, in X-ray Binaries, ed. W. H. G. Lewin, J. van Paradijs, & E. P. J. van den Heuvel (CUP), 58
Wade, R. A., & Horne, K. 1988, ApJ, 324, 411
Yi, I., & Narayan, R. 1997, ApJ, 486, 363
Zurita, C., Casares, J., & Shahbaz, T. 2003, ApJ, 582, 369